2

A quick review of gas dynamics

Before beginning a discussion of the special effects brought about by the energy and momentum of radiation, we review ideal gas dynamics as it exists without these sources. We will define the variables we use and present the main equations that will be modified later.

<mark>A quite good introduction to fluid mechanics is the volume *Fluid Mechanics* in the *Course of Theoretical Physics* by Landau and Lifshitz (1959).</mark> This does not spend much time on the microscopic picture of fluids, but is very strong on the physical applications. The approach is entirely analytic. Mihalas and Mihalas (1984) describe kinetic theory in some detail, and the basis of viscosity, in addition to some of the basic results of gas dynamics. The chapters on viscous effects and relativistic flows are valuable.

2.1 Ideal fluid description: ρ, p, $\mathbf{u}$, and e

A fluid is, as the name suggests, free to flow, which distinguishes it from an elastic solid. The solid can deform, but as it does stresses are produced that depend on the displacements. In a fluid the stress is primarily (i.e., apart from a small correction due to viscosity) an <mark>isotropic pressure, and this depends on the local temperature and density of the matter,</mark> and is independent of how far a parcel may have moved from its starting point. <mark>So density is the parameter that expresses how the kinematics will change the state of the matter.</mark> The density evolves as the fluid moves, and the volume occupied by a parcel of material changes. The motion is described by the fluid velocity, $\mathbf{u}$. This is a vector which is equal to the mass-weighted average of the individual velocities of all the particles contained in a microscopic cell surrounding the point in question. A coarse-graining assumption is applied in the fluid picture. The assumption is made that a cell size can be chosen that is infinitesimal compared with the scale of the fluid region, yet so large that the statistical uncertainty of averages over the atoms in the cell is negligible. Furthermore, we

5

assume that, if the cell is carried along with the fluid velocity, it has just the same atoms in it at the end of some time of interest as it has at the start. In other words, even though the individual atoms are flying around with velocities that may be large compared with the mean – the fluid velocity – the amount of net progress an atom makes is negligible compared with the cell size. Clearly, this requires that the mean free path between atom collisions is negligible compared with the cell size. Both because of the atom statistics and because the mean free path varies inversely with the density, the fluid approximation is valid at high densities and breaks down at low density. It fails, for example, in high-vacuum laboratory experiments and in the outer parts of the solar wind.

The ideal fluid we have been describing is characterized by its mass density ρ, its pressure p, which gives the momentum flux of the particles across any infinitesimal element of area, and by the internal energy per unit mass, e. This includes the kinetic energies of all the particles, but, since kinetic energy may be stored temporarily in atomic excitation, the excitation energy is included as well, to make a conserved quantity. Density, pressure, and internal energy are three of the thermodynamic functions. For a system with a fixed mass such as the cell we are considering, only two of these are independent, for example density and internal energy. The pressure can be calculated from the other two using the known equation of state of the material, and all the other thermodynamic functions such as temperature, entropy, Helmholtz free energy, etc., can be as well.

2.2 Euler's equations

The mass of all the particles in a cell is thus one conserved quantity. A second conserved quantity is the total momentum of the particles in the cell. This is conserved in the sense that its rate of change equals the net gain in momentum due to particles entering or leaving across the cell boundary, plus any body force that may exist such as gravity. The first of these terms is the surface integral of the pressure over the boundary. The third conservation law is for the internal energy in the cell. This is expressed by the first law of thermodynamics, which says that the change in the internal energy is the negative of the pressure times the rate of volume increase of the cell, plus the rate of any addition of heat to the cell by external agents. By applying a little calculus to the conservation laws, they can be expressed as differential equations, Euler's equations for an ideal fluid.

The mathematical form of the conservation laws differs depending on whether the time derivative is taken at a fixed point in inertial space (Eulerian picture) or following a given parcel of fluid (Lagrangian picture). The manipulation is

somewhat easier with the Eulerian form, but then the expression of a conservation law must include terms for the flux of the conserved quantity across a fixed cell boundary. For conservation of mass, conservation says that the rate of change of the mass in a space-fixed volume, V, is just the negative of the integral of the mass flux, $\rho \mathbf{u}$, over the surface S of V, i.e.,

$$\frac{d}{dt} \int_V \rho \, dV = - \int_S \rho \mathbf{u} \cdot d\mathbf{A}. \tag{2.1}$$

By making use of the divergence theorem, and requiring the relation to be true for every cell volume, we find the first Euler equation

$$\frac{\partial \rho}{\partial t} + \nabla \cdot (\rho \mathbf{u}) = 0. \tag{2.2}$$

The momentum conservation law follows in a similar way. Two additions are needed, however. The surface integral contains not only the flux of momentum, $-(\rho \mathbf{u})\mathbf{u} \cdot d\mathbf{A}$, being carried across the boundary, but also the momentum flux associated with pressure, $-p \, d\mathbf{A}$. Also, if there is a body force, it gives a momentum source rate F per unit volume. The result is the second Euler equation

$$\frac{\partial \rho \mathbf{u}}{\partial t} + \nabla \cdot (\rho \mathbf{u}\mathbf{u}) + \nabla p = F. \tag{2.3}$$

The divergence in the second term on the left-hand side needs a comment. This is the divergence of a tensor and the result is a vector. The tensor has two indices, one from each factor $\mathbf{u}$, and the divergence is taken by assigning first 1 to the second index, and forming the ordinary divergence of $\rho \mathbf{u} u_1$, then repeating for index 2 and index 3, thus obtaining the three components of the result.

The derivation of Euler's energy conservation law from the first law of thermodynamics is more roundabout. We have to begin with the notion of the time derivative taken following the motion of the fluid, the Lagrangian time derivative D/Dt, which is given by $Df/Dt = \partial f/\partial t + \mathbf{u} \cdot \nabla f$ for any function f. Secondly, we recognize that the volume occupied by a unit mass of material is $1/\rho$. The time rate of change of the volume of this fixed parcel of mass is $D(1/\rho)/Dt$. According to the first law of thermodynamics, the Lagrangian rate of change of the specific internal energy, plus the rate per unit mass at which the pressure is doing work, equals the rate per unit mass at which heat is being deposited from external sources, q. Thus the Lagrangian internal energy equation is

$$\frac{De}{Dt} + p\frac{D(1/\rho)}{Dt} = q \tag{2.4}$$

or

$$\frac{\partial e}{\partial t} + \mathbf{u} \cdot \nabla e + p\frac{\partial 1/\rho}{\partial t} + p\mathbf{u} \cdot \nabla(1/\rho) = q. \tag{2.5}$$

In order to make this look more like an Eulerian conservation law we make use of this handy identity for any function f:

$$\rho \frac{Df}{Dt} = \frac{\partial \rho f}{\partial t} + \nabla \cdot (\rho \mathbf{u} f), \tag{2.6}$$

which is easily proved by expanding the derivatives of the products and using the Eulerian mass conservation equation, (2.2). When this identity is applied to (2.4) multiplied by ρ, this form of the internal energy conservation law results:

$$\frac{\partial \rho e}{\partial t} + \nabla \cdot (\rho \mathbf{u} e) + p \nabla \cdot \mathbf{u} = \rho q. \tag{2.7}$$

This is still not an expression of "energy conservation" because of the pressure work term, $p \nabla \cdot \mathbf{u}$. In order to eliminate that, we first derive a mechanical energy conservation law by forming the dot product of the velocity with the momentum conservation equation, (2.3), and making use of mass conservation again. The result is

$$\frac{\partial}{\partial t} \left(\frac{1}{2} \rho u^2 \right) + \nabla \cdot \left(\frac{1}{2} \rho \mathbf{u} u^2 \right) + \mathbf{u} \cdot \nabla p = \mathbf{u} \cdot F. \tag{2.8}$$

The sum of the internal energy equation (2.7) and the mechanical energy equation (2.8) is the total energy equation

$$\frac{\partial}{\partial t} \left(\rho e + \frac{1}{2} \rho u^2 \right) + \nabla \cdot \left(\rho \mathbf{u} e + \frac{1}{2} \rho \mathbf{u} u^2 + p \mathbf{u} \right) = \rho q + \mathbf{u} \cdot F. \tag{2.9}$$

This is the form usually considered as the third Euler equation. The conserved quantity is the sum of the internal and the kinetic energies, and its flux has a part from advection with the fluid and another part due to the pressure. The effect of this pressure term is the same as replacing the internal energy flux by the flux of enthalpy, $h = e + p/\rho$.

The way that the three Euler equations are used to solve a hydrodynamic initial value problem is conceptually something like the following. The current values of the three conserved quantities, ρ, $\rho \mathbf{u}$, and $\rho e + 1/2 \rho u^2$ are solved for ρ, $\mathbf{u}$, and e. Given ρ and e, the equation of state supplies the pressure p. These are all the variables needed to determine the fluxes in the three conservation laws and the source terms, if any. From these values the three time derivatives are calculated, and the conserved quantities can be advanced to the next time step. Refined calculations may differ from this scheme in detail, but the concept is the same.

2.3 Lagrangian equations

If we imagine that at an initial time we draw a spatial mesh on the material that makes up our problem, and that subsequently this mesh is dragged along with the material as it moves, then we have the Lagrangian picture. The appropriate time derivative, at a fixed point in the Lagrangian mesh, is D/Dt, which we used above. When spatial derivatives are required in the equations they are with respect to ordinary fixed coordinates, and they have to be calculated first with respect to the dragged-along Lagrangian mesh, then transformed using the chain rule to the fixed-space variables. When the flow is highly rotational, not to mention turbulent, the Lagrangian mesh is increasingly distorted as time goes by, and eventually this transformation introduces so much error that the Lagrangian mesh can no longer be used. Thus in rotational problems (in the sense $\nabla \times \mathbf{u} \neq 0$) Lagrangian coordinates are limited-life components. In some cases, for example spherical symmetry, this problem never arises, and the Lagrangian mesh can be used indefinitely.

The main equations of the Lagrangian method have been mentioned already. Mass conservation deserves special mention. Because the mesh follows the material, conservation of mass is guaranteed. What is needed, however, is the formula to compute the density from the current mapping from Lagrangian space to fixed space. If we call our Lagrangian coordinates ξ, η, ζ, and the Eulerian coordinates x, y, and z, then the true volume of a cell corresponding to a Lagrangian volume $d\xi d\eta d\zeta$ is $dV = d\xi d\eta d\zeta \, \partial(x, y, z)/\partial(\xi, \eta, \zeta)$. The last factor is the Jacobian of the mapping. Since the mass of the cell is constant, the density varies exactly as the reciprocal of the Jacobian. It is not hard to show that the logarithmic time derivative of the Jacobian is exactly $\nabla \cdot \mathbf{u}$, as expected from $D\rho/Dt + \rho \nabla \cdot \mathbf{u} = 0$, another form of (2.2). The Lagrangian momentum equation is found by applying the identity (2.6) in reverse to the Eulerian momentum equation (2.3) to give

$$\frac{D\mathbf{u}}{Dt} + \frac{1}{\rho}\nabla p = \frac{F}{\rho}. \tag{2.10}$$

In practical calculations the total force is found by combining the specified volume force F and the pressure gradient term, of which the latter is obtained using the chain rule for differentiation as mentioned above. Then the total force, converted to an acceleration, is used to update the velocity of the Lagrangian mesh. The velocity is used to move the mesh to its position for the next time step. After the mesh is moved, the Jacobian of the mapping can be recalculated, and with it the densities of all the Lagrangian cells.

The energy update is done with the Lagrangian internal energy equation (2.4), which we have discussed already. The pdV term can be evaluated since the change in density is now known, and the result is a new internal energy for every cell.

This is enough information to enable the new pressures to be evaluated, and the calculation can proceed to the next time step.

2.4 Moving mesh – ALE

There are complementary advantages of the Eulerian and Lagrangian pictures. The Eulerian picture has the advantage of a regular mesh – often Cartesian – which makes it possible to construct relatively sophisticated finite-difference or finite-element numerical representations of the Euler equations. The truncation terms can be bounded, and adjustments to the time step or to the mesh can be made if the estimated error is too great. A disadvantage is that the advection terms in the equations (terms like $\mathbf{u} \cdot \nabla\rho$), absent in the Lagrangian picture, are hard to represent accurately, and Eulerian methods in the past often produced unacceptable smearing of contact discontinuities, interfaces carried along with the fluid that separate two different materials, or regions of different entropy and temperature or transverse component of velocity. In the Lagrangian picture contact discontinuities are not a problem, since the mesh follows the matter. The serious problem is that the mesh becomes progressively distorted as the calculation proceeds, and the accuracy of differencing in the distorted mesh is of a lower order. Eventually the distortion results in zones being turned inside out or otherwise grossly disturbed, and the calculation simply stops. At this point, a new mesh has to be created by hand, and all the fluid variables must be interpolated from the old, distorted mesh to the new one. This interpolation is by no means very accurate, not least since the operation is not applied until the mesh distortion is already severe. The accuracy in following contact discontinuities normally possessed by the Lagrangian method may all be lost in the interpolation process.

Modern techniques have improved both Lagrangian and Eulerian methods. Advances in numerical algorithms have produced treatments of the advection problem that allow sharp definition of contact discontinuities even as they propagate across many cells of the Eulerian mesh, with the result that advection is no longer the Achilles heel of Eulerian methods. Sophisticated rezoning techniques that are applied automatically within the code enable Lagrangian codes to keep running long after they would formerly have crashed. A general formulation that amounts to applying a rezoning operation every time step is called arbitrary Lagrangian Eulerian, or ALE. The idea is that the computational mesh moves with respect to fixed space with a velocity $\mathbf{v}_g$, a function of space and time that is whatever the hydrodynamics code, through an adaptive procedure, decides to make it. If $\mathbf{v}_g$ were zero, the method would be Eulerian; if $\mathbf{v}_g$ were the fluid velocity $\mathbf{u}$, the method would be Lagrangian. Since $\mathbf{v}_g$ is arbitrary, we have the name of the method. The ALE equations are found by replacing the Eulerian time derivative $\partial/\partial t$ with

$(\partial/\partial t)_g - \mathbf{v}_g \cdot \nabla$, where $(\partial/\partial t)_g$ is the time derivative at a fixed point in the mesh. The result is a set of Eulerian-like equations including extra terms involving $\mathbf{v}_g$:

$$\left(\frac{\partial \rho}{\partial t}\right)_g + \nabla \cdot [\rho(\mathbf{u} - \mathbf{v}_g)] = -\rho \nabla \cdot \mathbf{v}_g, \tag{2.11}$$

$$\left(\frac{\partial \rho \mathbf{u}}{\partial t}\right)_g + \nabla \cdot [\rho(\mathbf{u} - \mathbf{v}_g)\mathbf{u}] + \nabla p = F - \rho \mathbf{u} \nabla \cdot \mathbf{v}_g, \tag{2.12}$$

$$\left(\frac{\partial}{\partial t}\right)_g \left(\rho e + \frac{1}{2}\rho u^2\right) + \nabla \cdot \left[\rho(\mathbf{u} - \mathbf{v}_g)\left(e + \frac{1}{2}u^2\right) + p\mathbf{u}\right]$$
$$= \rho q + \mathbf{u} \cdot F - \rho \left(\frac{1}{2}u^2 + e\right)\nabla \cdot \mathbf{v}_g. \tag{2.13}$$

We see that the advection fluxes, instead of being proportional to the mass flux $\rho \mathbf{u}$, as in the Eulerian method, are proportional to the flux $\rho(\mathbf{u} - \mathbf{v}_g)$ that crosses the moving zone boundary. The residual terms in $\nabla \cdot \mathbf{v}_g$ are due to the changing volumes of the ALE zones.

We can make a useful transformation of these equations by introducing the definition $J = \partial(x, y, z)/\partial(\xi, \eta, \zeta)$ for the Jacobian of the mapping from ALE coordinates to Cartesian coordinates. The volume of an ALE zone varies with time in proportion to the local value of J. The product ρJ is proportional to the zone mass. The identity relating J and $\mathbf{v}_g$ is

$$\frac{1}{J}\left(\frac{\partial J}{\partial t}\right)_g = \nabla \cdot \mathbf{v}_g. \tag{2.14}$$

By introducing J as a factor in the time derivatives in (2.11)–(2.13) the $\nabla \cdot \mathbf{v}_g$ terms are absorbed, which gives the ALE equations:

$$\frac{1}{J}\left(\frac{\partial \rho J}{\partial t}\right)_g + \nabla \cdot [\rho(\mathbf{u} - \mathbf{v}_g)] = 0, \tag{2.15}$$

$$\frac{1}{J}\left(\frac{\partial \rho J \mathbf{u}}{\partial t}\right)_g + \nabla \cdot [\rho(\mathbf{u} - \mathbf{v}_g)\mathbf{u}] + \nabla p = F, \tag{2.16}$$

$$\frac{1}{J}\left(\frac{\partial}{\partial t}\right)_g \left[\rho J\left(e + \frac{1}{2}u^2\right)\right] + \nabla \cdot \left[\rho(\mathbf{u} - \mathbf{v}_g)\left(e + \frac{1}{2}u^2\right) + p\mathbf{u}\right] = \rho q + \mathbf{u} \cdot F. \tag{2.17}$$

There is a great deal of freedom in choosing $\mathbf{v}_g$, and ALE codes include sophisticated routines for making an optimum choice in which the goals of following the material and keeping the mesh regular and orthogonal, if possible, are balanced. The algorithms for doing this vary with the ALE code.

The numerical methods used to solve this set of equations are much like those for the Eulerian method, which are too varied to discuss here. A strategy often used for both Eulerian and ALE codes is to break the time step into two parts: a first part in which the advection fluxes are dropped, i.e., a pure Lagrangian step, followed by a remap process that accounts for the amount of advection during the time step.

2.5 Transport terms: viscosity and heat conduction

So far we have considered ideal fluids for which we can completely ignore the possibility that individual atoms may migrate from a fixed position with respect to the mean fluid. In reality, of course, the atoms travel a nonzero distance between collisions, and so the atoms that populate any small parcel of fluid had their last collisions some finite distance away, in various random directions. This means that the local velocity distribution function may not be exactly isotropic, but will include fluctuations related to the gradients of temperature and fluid velocity. For example, if the fluid velocity component u_y is increasing in the x direction, an atom that arrives in the parcel traveling generally in the $+x$ direction will have a u_y value that is biased negatively compared with the average value in the parcel. The amount of bias is of the order of the mean free path times the x-gradient of u_y. Alternatively, if the temperature is increasing in the x direction, that atom that arrives in the parcel traveling generally toward $+x$ will have a small negative bias in its kinetic energy. When these biases are evaluated using an accurate kinetic theory model, what result are corrections (viscous stress) to the ideal pressure and a nonzero heat flux.

The viscous stress and the conductive heat flux are expressed in terms of coefficients that are either empirical constants or derived from kinetic theory. For terrestrial gases and liquids the values are tabulated in handbooks; for plasmas and for conditions very different from those realizable on earth, theoretical values must be used. Viscosity results in the replacement of the isotropic pressure with a stress tensor:

$$p\delta_{ij} \rightarrow P_{ij} = p\delta_{ij} - \sigma_{ij}, \tag{2.18}$$

in component notation (i and j are free indices running from 1 to 3), and δ_{ij} is the Kronecker delta, 1 if $i = j$ and 0 otherwise. The viscous stress σ_{ij} is determined by the rate-of-strain tensor according to

$$\sigma_{ij} = \mu \left(u_{i,j} + u_{j,i} - \frac{2}{3} u_{k,k} \delta_{ij} \right) + \zeta u_{k,k} \delta_{ij}. \tag{2.19}$$

(In tensor component equations like this a subscript following a comma indicates differentiation by the coordinate with that index, and a repeated index, such as k in this case, is to be summed over.) The coefficient μ is the (ordinary) coefficient of viscosity, and ζ is the coefficient of bulk viscosity. The inclusion of the ζ term often causes a lengthy discussion, since there are some good reasons for thinking it should be zero, and the kinetic theory models generally give a zero value. Experimental measurements of the bulk viscosity are elusive, because its effect vanishes in an incompressible flow where $u_{k,k} = \nabla \cdot \mathbf{u} = 0$, and compressible flows are generally high-velocity flows, for which the Reynolds number is large and viscous effects are therefore unimportant. The order of magnitude of μ is ρ times the mean thermal speed of an atom times the atomic mean free path. Because the mean free path is proportional to the reciprocal of the atomic cross section times the number density of atoms, the density factors cancel out in the coefficient of viscosity, which should therefore be nearly independent of density, though varying somewhat with temperature.

Including the viscous stress in Euler's momentum conservation equation leads to the first form of the Navier–Stokes equation:

$$\frac{\partial \rho \mathbf{u}}{\partial t} + \nabla \cdot (\rho \mathbf{uu}) + \nabla p = F + \nabla \cdot \{\mu[\nabla \mathbf{u} + (\nabla \mathbf{u})^{\mathrm{T}}]\} + \nabla \left[\left(\zeta - \frac{2}{3}\mu \right) \nabla \cdot \mathbf{u} \right].$$

$$(2.20)$$

The notation for the tensor components that is used here is that if i is the row index and j is the column index, so that the divergence operation involves summing on i, then the components of $\nabla \mathbf{u}$ are $u_{i,j}$ and those of its transpose, $\nabla \mathbf{u}^{\mathrm{T}}$, are $u_{j,i}$.

As mentioned above, the viscosity coefficients are not too strongly dependent on the state of the material. If this dependence is neglected, then the coefficients can be taken outside the spatial derivatives to give the second form of the Navier–Stokes equation:

$$\frac{\partial \rho \mathbf{u}}{\partial t} + \nabla \cdot (\rho \mathbf{uu}) + \nabla p = F + \mu \nabla^2 \mathbf{u} + \left(\zeta + \frac{1}{3}\mu \right) \nabla \nabla \cdot \mathbf{u}, \qquad (2.21)$$

and since we are frequently interested in viscous effects when the flow is incompressible ($\nabla \cdot \mathbf{u} = 0$), we have the third form:

$$\frac{\partial \rho \mathbf{u}}{\partial t} + \nabla \cdot (\rho \mathbf{uu}) + \nabla p = F + \mu \nabla^2 \mathbf{u}. \qquad (2.22)$$

There are no viscous effects for mass conservation, since the fluid velocity is defined as the mean mass flux divided by the density. The viscous term in the energy equation will be considered after heat conduction is discussed. Thermal

conduction is very simple; Fourier's law is

$$F_{\text{heat}} = -K\nabla T. \tag{2.23}$$

The thermal conductivity K is tabulated in handbooks for terrestrial materials, and estimated theoretically using methods of kinetic theory or condensed matter theory for others. The magnitude of K is approximately the mass density times the specific heat at constant volume times the atomic mean free path. So for gases, the thermal conductivity and viscosity are closely related. Anticipating some of the later discussion, we note that the ratio of the diffusivity of momentum, μ/ρ, to the diffusivity of heat, $K/(\rho C_p)$, defines the Prandtl number, and that for a hard-sphere monatomic gas it has the value 2/3. The effect of heat conduction on the energy equation is to add a volume energy source $-\nabla \cdot F_{\text{heat}}$ to the right-hand side. The effect of viscosity on the energy equation comes because the rate of doing work by the viscous stress subtracts from the internal energy. The term $p\nabla \cdot \mathbf{u}$ in (2.7) is modified by subtracting $\Phi = \sigma_{ij}u_{i,j}$, where a sum over i and j is implied. This quantity Φ is called the dissipation function, and can be written as

$$\Phi = \frac{1}{2}\mu(u_{i,j} + u_{j,i})(u_{i,j} + u_{j,i}) + \left(\zeta - \frac{2}{3}\mu\right)(\nabla \cdot \mathbf{u})^2. \tag{2.24}$$

The dissipation function is never negative. The μ part is nonnegative, and vanishes if and only if the strain rate is isotropic, i.e., uniform dilation. The ζ part is also nonnegative (for $\zeta > 0$) and vanishes if and only if the bulk expansion $\nabla \cdot \mathbf{u}$ vanishes. The internal energy equation (2.7) is therefore modified to

$$\frac{\partial \rho e}{\partial t} + \nabla \cdot (\rho \mathbf{u}e) + p\nabla \cdot \mathbf{u} = \rho q + \Phi + \nabla \cdot (K\nabla T). \tag{2.25}$$

The left-hand side can also be written $\rho[De/Dt + pD(1/\rho)/Dt]$, which is equal to $\rho Ds/Dt$, where s is the specific entropy. From this we see that the viscous dissipation function Φ always acts to increase the entropy. With the inclusion of both viscosity and heat conduction, the total energy conservation equation becomes

$$\frac{\partial}{\partial t}\left(\rho e + \frac{1}{2}\rho u^2\right) + \nabla \cdot \left\{\rho \mathbf{u}e + \frac{1}{2}\rho \mathbf{u}u^2 + p\mathbf{u}\right.$$
$$\left. -\mu\left[\mathbf{u}\cdot\nabla\mathbf{u} + \nabla\left(\frac{1}{2}u^2\right)\right] - \left(\zeta - \frac{2}{3}\mu\right)(\nabla \cdot \mathbf{u})\mathbf{u} - K\nabla T\right\}$$
$$= \rho q + \mathbf{u}\cdot F, \tag{2.26}$$

where now q refers to heat deposition other than from thermal conduction, and F continues to be the externally applied force per unit volume.

2.6 Bernoulli's equation and applications

A couple of simple manipulations of Euler's equations give results that are very useful for applications. The first is Bernoulli's equation. We begin by observing this identity for the velocity gradient term in the acceleration equation:

$$\mathbf{u} \cdot \nabla \mathbf{u} = \nabla \frac{1}{2} u^2 - \mathbf{u} \times \nabla \times \mathbf{u}. \tag{2.27}$$

Furthermore, suppose that the external force F is a body force derived from a potential, V, viz., $F = -\rho \nabla V$. Then the acceleration equation becomes

$$\frac{\partial \mathbf{u}}{\partial t} + \nabla \left(\frac{1}{2} u^2 \right) - \mathbf{u} \times \nabla \times \mathbf{u} + \frac{1}{\rho} \nabla p + \nabla V = 0. \tag{2.28}$$

In the case of steady flow, when all the variables are time-independent, we can drop the $\partial \mathbf{u}/\partial t$ term, then form the dot product of this equation with $\mathbf{u}$, and obtain

$$\mathbf{u} \cdot \nabla \left(\frac{1}{2} u^2 + \int \frac{dp}{\rho} + V \right) = 0, \tag{2.29}$$

which says that the quantity in parentheses has a constant value on any given streamline. This is the weak form of Bernoulli's law. It is useful if there is a functional relation between p and ρ (barotropic law) such as is provided in adiabatic flow or isothermal flow. In the adiabatic case the integral $\int dp/\rho$ becomes the enthalpy and in the isothermal case it becomes the Gibbs free energy, for example.

A stronger form of Bernoulli's law results for irrotational flows, i.e., flows for which the vorticity, $\nabla \times \mathbf{u}$, vanishes. As we know from electrostatics, when $\nabla \times \mathbf{u}$ vanishes globally $\mathbf{u}$ can be derived from a potential, $\mathbf{u} = \nabla \phi$. Making this replacement and dropping the vorticity term in (2.28) leads to

$$\nabla \left(\frac{\partial \phi}{\partial t} + \frac{1}{2} u^2 + \int \frac{dp}{\rho} + V \right) = 0, \tag{2.30}$$

which says that the quantity in parentheses is constant in all space, though it may vary with time. If the flow is both steady and irrotational, the $\partial \phi/\partial t$ term may be dropped, which then says that the same Bernoulli constant as in the weak form is in fact uniform over all space, not just on a streamline.

Potential flow is the name for flows that are both irrotational and incompressible. By virtue of the first assumption we can write $\mathbf{u} = \nabla \phi$; by virtue of the second we can require $\nabla \cdot \mathbf{u} = 0$, so the velocity potential ϕ must satisfy Laplace's equation $\nabla^2 \phi = 0$. The problem is virtually solved at that point, since we can use the methods of potential theory, boundary-value problems and the like, to find the solution for ϕ. The pressure need not even be considered in this procedure, depending on the boundary conditions. As a last step, Bernoulli's equation in its

strong form is used to find the pressure. Incompressible flow is always barotropic since $\int dp/\rho = p/\rho$ when ρ is uniform and constant.

As mentioned above, the vorticity is defined by $\boldsymbol{\omega} = \nabla \times \mathbf{u}$. A helpful equation for understanding vorticity is found by taking the curl of the Eulerian acceleration equation (2.28):

$$\frac{\partial \boldsymbol{\omega}}{\partial t} - \nabla \times (\mathbf{u} \times \boldsymbol{\omega}) - \frac{\nabla \rho \times \nabla p}{\rho^2} = \nabla \times \frac{F}{\rho}. \qquad (2.31)$$

This is an interesting equation, since it says that vorticity cannot be produced in a barotropic flow that has an external body force derived from a potential, if any. This is because the barotropic relation $p = f(\rho)$ implies that ∇p is parallel to $\nabla \rho$, and therefore the cross product term, called the baroclinic term, vanishes. The integral Γ of the vorticity over a surface S bounded by a curve C is called the circulation around C, since by Stokes's theorem,

$$\Gamma = \int_S \boldsymbol{\omega} \cdot d\mathbf{A} = \oint_C \mathbf{u} \cdot d\mathbf{l}. \qquad (2.32)$$

It is a calculus exercise to show that the equation

$$\frac{\partial \boldsymbol{\omega}}{\partial t} = \nabla \times (\mathbf{u} \times \boldsymbol{\omega}) \qquad (2.33)$$

obtained by dropping the baroclinic term and the external force term implies that Γ is constant in time for any curve C that is carried along by the fluid. In this sense, vorticity is a conserved quantity in the absence of the generation terms.

Vorticity is also the basis of numerical methods for incompressible hydrodynamics. Using the analogy $\mathbf{u}$ is to $\boldsymbol{\omega}$ as magnetic induction $\mathbf{B}$ is to current density $\mathbf{J}$, appropriate for the incompressible case, $\mathbf{u}$ can be reconstituted from $\boldsymbol{\omega}$. Thus we can regard $\boldsymbol{\omega}$ as the basic unknown and derive $\mathbf{u}$ from it, then use the vorticity equation to update the vorticity, i.e., move the vortices. Vortex dynamics is the name for the method that uses this approach with a finite set of line vortices. This approach is outstandingly successful in modeling Jupiter's Great Red Spot, to pick one example. (See Marcus (1993).)

Even in a flow that has quite a high Reynolds number, and for which, therefore, the viscous effects should be quite small, there may be viscous boundary layers, since the flow solution in the interior of the problem, which is essentially inviscid, may not obey the true boundary conditions. An example is flow over a surface, where the flow velocity must be zero at the surface, but is some finite value a moderate distance away. In this case a rapid transition occurs in a layer next to the surface to join the interior solution to the required boundary condition. The thickness of the transition layer is proportional to the small viscosity, since only by having a large gradient can the small viscosity term have a macroscopic effect.

These boundary layers can act as producers of vorticity, which then is transported into the bulk downstream flow.

Deposition of heat is another mechanism by which vorticity can be generated. The addition of heat can easily have a spatial dependence that results in the pressure no longer being strictly a function of the density. Once this occurs there is baroclinic vorticity production. As we shall see, the same is true of shock waves. A shock wave that is not uniform in the transverse direction results in an entropy increase that has a transverse gradient, and therefore a nonzero baroclinic term.

As an example of the use of the method of potential flow and the strong form of Bernoulli's law, we consider the case of two superposed incompressible fluids, possibly of different densities, which may also be in relative horizontal motion, and acted upon by vertical gravity. When the fluid interface is perturbed slightly, surface waves, or possibly instabilities may be produced. The waves are deep-water waves, and the instabilities are Rayleigh–Taylor or Kelvin–Helmholtz, depending on the setup.

The unperturbed state is of density ρ_1 for $z > 0$ and density ρ_2 for $z < 0$, and a velocity in the x direction of U_1 for $z > 0$ and U_2 for $z < 0$. The perturbed surface is displaced by a small amount z_s in the z direction, which we take to be $\zeta \exp(i\mathbf{k}_h \cdot \mathbf{r} - i\omega t)$. The vector $\mathbf{k}_h$ has only x and y components, and we are looking for the dispersion relation that gives ω in terms of $\mathbf{k}_h$. A real ω means surface waves; a complex ω with a positive imaginary part means an unstable interface.

In the unperturbed state, the pressure is uniform across the plane $z = 0$, and has the same value on either side of the interface. We will take this as the zero of pressure. When the surface is perturbed, a flow exists in both $z > 0$ and $z < 0$, but we expect the flow in each region to be irrotational. If U_1 and U_2 are different, there is a vortex sheet at $z = 0$ in the unperturbed state, and we will see that even when U_1 and U_2 are equal, vorticity may develop on the perturbed interface. So the solution we are looking for is a potential flow in each region, for which we then require matching on the interface. The quantities that have to match at the interface are the normal component of velocity and the pressure.

We let ϕ_1 and ϕ_2 be the velocity potentials in the respective regions. Each of these satisfies Laplace's equation. Since we have chosen the interface perturbation to have the horizontal variation $\exp(i\mathbf{k}_h \cdot \mathbf{r})$, the appropriate harmonic functions are $\exp(\pm k_h z + i\mathbf{k}_h \cdot \mathbf{r})$, where k_h is the vector magnitude of $\mathbf{k}_h$. Since the fluctuations should vanish far from the interface, we choose the $-$ sign for $z > 0$ and the $+$ sign for $z < 0$. To these are added the potentials corresponding to the unperturbed uniform flows, $U_1 x$ or $U_2 x$. Thus we put

$$\phi = \begin{cases} U_1 x + \psi_1 \exp(-k_h z + i\mathbf{k}_h \cdot \mathbf{r} - i\omega t) = \phi_1, & z > 0, \\ U_2 x + \psi_2 \exp(k_h z + i\mathbf{k}_h \cdot \mathbf{r} - i\omega t) = \phi_2, & z < 0. \end{cases} \tag{2.34}$$

The normal velocity matching proceeds as follows. The direction of the surface normal is the vector

$$-ik_x\zeta \exp(i\mathbf{k}_h \cdot \mathbf{r} - i\omega t)\mathbf{e}_x - ik_y\zeta \exp(i\mathbf{k}_h \cdot \mathbf{r} - i\omega t)\mathbf{e}_y + \mathbf{e}_z. \quad (2.35)$$

The vectors $\mathbf{e}_x$, $\mathbf{e}_y$ and $\mathbf{e}_z$ are unit vectors in the three coordinate directions. The component along the normal of the velocity of the interface is just $\partial z_s/\partial t$ to first order, or

$$-i\omega\zeta \exp(i\mathbf{k}_h \cdot \mathbf{r} - i\omega t). \quad (2.36)$$

The fluid velocity in region 1 at the interface is

$$(U_1 + ik_x\psi_1 \exp(i\mathbf{k}_h \cdot \mathbf{r} - i\omega t))\mathbf{e}_x + ik_y\psi_1 \exp(i\mathbf{k}_h \cdot \mathbf{r} - i\omega t)\mathbf{e}_y$$
$$-k_h\psi_1 \exp(i\mathbf{k}_h \cdot \mathbf{r} - i\omega t)\mathbf{e}_z. \quad (2.37)$$

Taking the component of this along the normal vector gives a part from U_1 due to the tilt of the surface in addition to the vertical component of the fluid velocity, i.e.,

$$-ik_x\zeta \exp(i\mathbf{k}_h \cdot \mathbf{r} - i\omega t)U_1 - k_h\psi_1 \exp(i\mathbf{k}_h \cdot \mathbf{r} - i\omega t). \quad (2.38)$$

Matching this to the velocity of the interface gives

$$-i\omega\zeta = -k_h\psi_1 - ik_xU_1\zeta. \quad (2.39)$$

Repeating the argument for region 2 gives

$$-i\omega\zeta = k_h\psi_2 - ik_xU_2\zeta. \quad (2.40)$$

Next we have to evaluate the pressure approaching the interface from each of the two sides, and match them. In each region the pressure follows from the strong form of Bernoulli's law, which gives

$$p = -\rho\left(gz + \frac{\partial\phi}{\partial t} + \frac{1}{2}u^2 - \frac{1}{2}U_\infty^2\right) \quad (2.41)$$

in each region separately. Here U_∞ is U_1 or U_2, as appropriate. This additive constant has been chosen to ensure that p matches the unperturbed value $-\rho gz$ far from the interface. We put in (2.34) for ϕ and $\mathbf{u} = \nabla\phi$, and expand, dropping the second order terms. Then setting $z = 0$ we get the upper-side and lower-side interface pressures:

$$p(0+) = -\rho_1(g\zeta - i\omega\psi_1 + U_1ik_x\psi_1)\exp(i\mathbf{k}_h \cdot \mathbf{r} - i\omega t), \quad (2.42)$$
$$p(0-) = -\rho_2(g\zeta - i\omega\psi_2 + U_2ik_x\psi_2)\exp(i\mathbf{k}_h \cdot \mathbf{r} - i\omega t). \quad (2.43)$$

We next equate these two expressions to each other, and substitute for ψ_1 and ψ_2 from (2.39) and (2.40). Canceling the factor ζ and the exponential then gives the dispersion relation

$$(\rho_2 - \rho_1)g - \rho_1 \frac{(\omega - k_x U_1)^2}{k_h} - \rho_2 \frac{(\omega - k_x U_2)^2}{k_h} = 0. \tag{2.44}$$

When this is arranged as a quadratic equation in ω, it becomes

$$(\rho_1 + \rho_2)\omega^2 - 2k_x(\rho_1 U_1 + \rho_2 U_2)\omega + k_x^2(\rho_1 U_1^2 + \rho_2 U_2^2) - (\rho_2 - \rho_1)k_h g = 0. \tag{2.45}$$

Solving it, we get

$$\omega = k_x \frac{\rho_1 U_1 + \rho_2 U_2}{\rho_1 + \rho_2} \pm \sqrt{\frac{\rho_2 - \rho_1}{\rho_1 + \rho_2} k_h g - k_x^2 \frac{\rho_1 \rho_2 (U_1 - U_2)^2}{(\rho_1 + \rho_2)^2}}. \tag{2.46}$$

This is the main result. We can directly apply it to three different problems. The first is deep-water waves, for which ρ_1 is negligible (since region 1 is air) and U_1 and U_2 are both zero. The dispersion relation gives real frequencies $\omega = \pm\sqrt{k_h g}$. These are dispersive waves, and the phase velocity $V_p = \omega/k_h = \sqrt{g/k_h}$ increases with the wavelength. The group velocity $d\omega/dk_h = 1/2\sqrt{g/k_h}$ is half the phase velocity. So for a wave packet of water waves, the wave crests appear at the rear of the packet, ride up over the top, and disappear at the front.

The second case is Rayleigh–Taylor instability, for which $\rho_1 > \rho_2$ and $U_1 = U_2 = 0$. The values of ω are imaginary, and in particular one root is $\omega = i\sqrt{(\rho_1 - \rho_2)k_h g/(\rho_1 + \rho_2)}$. This root leads to exponential growth in time with a growth rate given by the square root factor. We see that the rate depends on the Atwood number $\alpha = (\rho_1 - \rho_2)/(\rho_1 + \rho_2)$, which is a positive number less than 1. The growth rate depends only on the vector magnitude of k_h, so any planform z_h that satisfies $(\nabla_h^2 + k_h^2)z_h = 0$, whether rolls, checkerboard or Bessel function, will lead to the same growth rate.

The third case is the Kelvin–Helmholtz instability, with $\rho_1 = \rho_2$ and $U_1 \neq U_2$. The roots are imaginary, and the growth rate is $(1/2)k_x|\Delta U|$. The analysis here, it must be remembered, has neglected viscosity and surface tension, among other things. These dissipative effects will stabilize the instabilities if the wavenumbers are high, for this increases their relative importance.

A final remark concerns the vorticity in the Rayleigh–Taylor problem. All the vorticity lies in the interface itself; it is a vortex sheet. But at the initial time the amount of vorticity is negligible. As the instability grows, however, a shear develops across the interface since ψ_1 and ψ_2 have opposite signs, as we see from (2.39) and (2.40). So we have zones of positive and negative vorticity in the interface that exponentiate in magnitude with time, along with the size of the interface

perturbation. The total vorticity may remain nearly zero, but the positive and negative accumulations both increase. Eventually this shear helps amplify the instability, as in the Kelvin–Helmholtz case. This example helps illustrate the point that vorticity can be created in a problem through the action of discontinuities or the boundaries.

2.7 Sound waves

We will illustrate how to derive linear waves from the Euler equations. As more physical processes are added to the equations, the character of the waves changes, and perhaps new wave modes appear; exploring these is a way of gaining insight into the consequences of those new processes. A systematic presentation of the interaction of waves with radiation is contained in Chapter 8 of Mihalas and Mihalas (1984).

For the simplest possible waves, suppose we have a base state consisting of a uniform medium at rest, and we suppose that this state is perturbed by small amounts in density, velocity, and pressure, and suppose further that a barotropic relation $p \sim \rho^\gamma$ describes the variations. Let ρ' and p' be the fluctuations in density and pressure, and $\mathbf{u}$ itself is the fluctuation in velocity since the base state is at rest. We linearize the continuity and momentum equations by Taylor-expanding around the base state, and discard all terms of second or higher order in the fluctuations. The flow variables for the base state will keep their usual names after linearizing, since there is no possibility of confusing them with the fluctuations. The continuity equation becomes

$$\frac{\partial \rho'}{\partial t} + \rho \nabla \cdot \mathbf{u} = 0, \tag{2.47}$$

and the momentum equation becomes

$$\frac{\partial \mathbf{u}}{\partial t} + \frac{\gamma p}{\rho^2} \nabla \rho' = 0. \tag{2.48}$$

Now we seek sinusoidal wave solutions that are proportional to the complex exponential factor $\exp(i\mathbf{k} \cdot \mathbf{r} - i\omega t)$. That is, we can replace the time derivative operator by $-i\omega$ and the gradient operator by $i\mathbf{k}$. After doing this, our two equations turn into this 4×4 linear system for ρ' and the three components of $\mathbf{u}$:

$$\begin{pmatrix} -\omega & \rho \mathbf{k}^{\mathrm{T}} \\ (\gamma p/\rho^2)\mathbf{k} & -\omega \end{pmatrix} \begin{pmatrix} \rho' \\ \mathbf{u} \end{pmatrix} = 0, \tag{2.49}$$

where $\mathbf{k}$ stands for the wave vector as a column vector, $\mathbf{k}^{\mathrm{T}}$ is its transpose, a row vector, and is the 3×3 identity matrix. In order for a wave mode to exist, this

homogeneous linear system must have a nonzero solution, which means that its determinant, the dispersion function $D(\mathbf{k}, \omega)$, must vanish. The determinant is evaluated by adding $\rho k_x/\omega$ times the second row plus $\rho k_y/\omega$ times the third row plus $\rho k_z/\omega$ times the fourth row to the first row, which eliminates all the elements of $\rho \mathbf{k}^T$ in that row. Then expanding by the elements in the first row, as modified, gives

$$D(\mathbf{k}, \omega) = \left(-\omega + \frac{\gamma p}{\rho} \frac{\mathbf{k} \cdot \mathbf{k}}{\omega} \right)(-\omega^3) = \omega^2 \left(\omega^2 - \frac{\gamma p}{\rho} k^2 \right). \qquad (2.50)$$

We write scalar k for the magnitude of the vector $\mathbf{k}$. We use this dispersion relation in the following way. Let $\mathbf{k}$ be any real vector. Then solve $D(\mathbf{k}, \omega) = 0$ for the roots, ω. Since D is fourth order in ω, there are four roots, corresponding to the four flow variables ρ, u_x, u_y, and u_z. Each root gives a wave mode. However, the pair $\omega = \pm\sqrt{\gamma p/\rho}\,k$ represent the two directions of propagation for this $\mathbf{k}$ and are thus considered together as one mode. The wave speed is the barotropic sound speed $c = \sqrt{\gamma p/\rho}$. The degenerate $\omega = 0$ modes exist because the two possible transverse polarizations do not produce any density fluctuation and therefore no restoring force. We can find the mode shape, i.e., the proportionality of ρ', u_x, u_y, and u_z for that mode, by substituting values of ω and $\mathbf{k}$ that obey the dispersion relation into (2.49) and solving for the amplitudes. For the nondegenerate modes in this case we get

$$\mathbf{u} = c^2 \frac{\rho'}{\rho} \frac{\mathbf{k}}{\omega} = c \frac{\rho'}{\rho} \frac{\mathbf{k}}{k}, \qquad (2.51)$$

so the mode is longitudinal and the velocity fluctuation is the sound speed times the fractional density fluctuation.

For a given mode, the phase velocity vector is in the direction of $\mathbf{k}$ with the magnitude of ω/k. For the case of the positive root, this is c. The group velocity is the gradient of ω with respect to $\mathbf{k}$, where ω is considered as a function of $\mathbf{k}$ and is evaluated on a consistent branch of the multivalued function. For the positive ω branch, this also is a vector of magnitude c in the direction of $\mathbf{k}$, the same as the phase velocity. They agree because these sound waves are not dispersive.

For a second example we will include the energy equation instead of assuming the barotropic relation, and suppose that there is a Newton's cooling type of coupling to an external heat bath, perhaps by means of radiation. (See Mihalas and Mihalas (1984), Section 101.) This means that the heat deposition term is proportional to the negative of the temperature fluctuation. We will use the ideal gas relation $e = p/[(\gamma - 1)\rho]$, and take q to be given by

$$q = \frac{e}{\tau} \left(\frac{\rho'}{\rho} - \frac{p'}{p} \right) = \frac{1}{(\gamma - 1)\tau} \left(\frac{p\rho'}{\rho^2} - \frac{p'}{\rho} \right). \qquad (2.52)$$

The quantity τ, with dimension time, is the time constant for the temperature to relax to that of the heat bath.

The linearization of the internal energy equation (2.7) multiplied by $\gamma - 1$ gives

$$-i\omega \left(\frac{p'}{\rho} - \frac{p}{\rho^2} \rho' \right) + i\omega \frac{\rho'}{\rho^2} p (\gamma - 1) = (\gamma - 1) q = \frac{1}{\tau} \left(\frac{p\rho'}{\rho^2} - \frac{p'}{\rho} \right). \quad (2.53)$$

We can add this as a fifth equation to the previous set of four, and treat p' and ρ' as independent variables. Expanding the 5×5 determinant leads to a dispersion function that is fifth order in ω and second order in $\mathbf{k}$. A somewhat shorter route to the dispersion relation is to solve the linearized energy equation for the ratio p'/ρ', namely

$$\frac{p'}{\rho'} = \frac{p}{\rho} \frac{\gamma \omega \tau + i}{\omega \tau + i}, \quad (2.54)$$

in other words, exactly as if γ were replaced by the rational function

$$\frac{\gamma \omega \tau + i}{\omega \tau + i}. \quad (2.55)$$

The physical significance of this function is that the effective γ tends to 1 when the wave period is long compared with the cooling time constant, since then the oscillations are nearly isothermal, and it tends to the usual value when the period is much less than the cooling time constant, since there is too little time for any cooling to occur, and the oscillations are nearly adiabatic. When the effective γ is substituted into the dispersion relation for the acoustic modes we find, after clearing the linear function of ω in the denominator,

$$(\omega \tau + i)\omega^2 - \frac{c^2}{\gamma} (\gamma \omega \tau + i) k^2 = 0. \quad (2.56)$$

This cubic equation for ω has two roots that belong to the acoustic mode, and a single root that represents the cooling mode. We make this into a real, nondimensional equation by introducing a variable $\xi = i\omega\tau$. The equation for ξ is then

$$\xi^3 - \xi^2 + (kc\tau)^2 \xi - \frac{(kc\tau)^2}{\gamma} = 0. \quad (2.57)$$

The exact roots of this cubic are messy (illustrated in Figure 2.1), but the roots are easily discussed in the limits of large and small $kc\tau$. When $kc\tau$ is large, which is the high-frequency limit, then one approximate root will be found by balancing the third and fourth terms in the polynomial, and the other two come from approximately balancing the first and third terms. The first gives $\xi \approx 1/\gamma$, or $\omega \approx -i/(\gamma\tau)$. The other two are $\xi \approx \pm ikc\tau$, or $\omega \approx \pm kc$. So this is an adiabatic sound wave, and a cooling mode in which the specific heat at constant pressure,
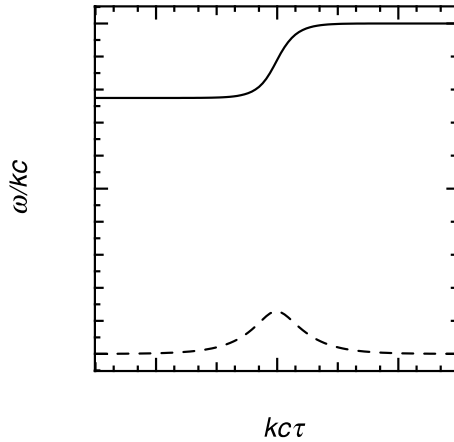
Fig. 2.1   Real and imaginary frequencies for sound waves with Newton's cool-
ing. Ordinate, ω scaled by kc; abscissa, cooling time in units of $1/kc$. Solid line,
real part; dashed line, imaginary part.

not constant volume, gives the decay time. This mode occurs at constant pressure
since it is slow compared with the sound propagation time.

In the limit of small $kc\tau$ one approximate root comes from balancing the first
and second terms, and the other two come from balancing the second and fourth.
The first is thus $\xi \approx 1$, or $\omega \approx -i/\tau$, and the other two are $\xi \approx \pm ikc\tau/\sqrt{\gamma}$, or
$\omega \approx \pm kc/\sqrt{\gamma}$. So in this low-frequency limit, the sound wave is isothermal, and
the cooling mode uses the specific heat at constant volume, since cooling occurs
too quickly for any motion to affect it.

The cooling term causes the sound wave to be damped; the roots for ω have a
small negative imaginary part. To see this, we apply one step of Newton–Raphson
iteration to account for the terms in the cubic that were neglected in the previous
paragraph. For the $kc\tau$ large case, we get

$$\omega \approx kc - i\frac{\gamma - 1}{\gamma\tau}, \tag{2.58}$$

while for the small $kc\tau$ case the result is

$$\omega \approx \frac{kc}{\sqrt{\gamma}} - i\frac{\gamma - 1}{2\gamma}(kc)^2\tau. \tag{2.59}$$

Interestingly, the damping is small in both the case of no cooling and the case of
strong cooling. Maximum damping occurs when the cooling time and the wave
period are comparable.

All this analysis can be used virtually intact if we replace Newton's cooling,
due perhaps to coupling with a radiation bath, with thermal conductivity. The only

difference is that the time constant τ is replaced with $1/(k^2\kappa) = \rho C/(k^2 K)$. Here K is the thermal conductivity, C is the specific heat, and κ is the corresponding thermal diffusivity. The dimensionless parameter $kc\tau$ becomes $c/(k\kappa)$. The roles of long and short wavelengths are now reversed. Heat conduction has the largest effect for short wavelengths, since the diffusion of heat increases faster with k than the frequency does. So the long-wavelength limit is the adiabatic one, and the short-wavelength limit is isothermal.

Space does not permit analyzing any more dispersion relations, but this technique is a powerful one for aiding the understanding of complicated hyperbolic systems.

2.8 Characteristics and simple waves

The method of characteristics for solving hyperbolic partial differential equations (PDEs) is primarily helpful for analytic studies of the properties of the systems, and not so much for practical computations. (The exception is Godunov's method – see below.) It is also a 1-D method. Characteristics in two and three dimensions are of a different nature than those in one dimension, and will not be discussed. Characteristics are very well explained by Courant and Friedrichs (1948), as are deflagration and detonation waves, which are analogous to ionization fronts, to be discussed in the last chapter of the present work.

A 1-D hyperbolic system of partial differential equations is represented as follows:

$$\frac{\partial U}{\partial t} + \frac{\partial F(U)}{\partial x} = G, \tag{2.60}$$

where U is a vector of unknowns, and F is a vector whose elements are functions of the elements of U. The definition of a characteristic is a curve in space-time along which a total differential equation involving elements of U is obeyed.

Here is how we find the characteristics of a system like (2.60). We expand the derivative of F using the chain rule:

$$\frac{\partial U}{\partial t} + A\frac{\partial U}{\partial x} = G, \tag{2.61}$$

where now A is the square Jacobian matrix $\partial F/\partial U$. Suppose we can find a left eigenvector $\mathbf{m}^T$ of A, a row vector, so that

$$\mathbf{m}^T A = c\mathbf{m}^T, \tag{2.62}$$

where c is a scalar that has dimensions of velocity. Multiplying (2.61) from the left by $\mathbf{m}^{\mathrm{T}}$ gives

$$\mathbf{m}^{\mathrm{T}} \left(\frac{\partial U}{\partial t} + c \frac{\partial U}{\partial x} \right) = \mathbf{m}^{\mathrm{T}} G. \tag{2.63}$$

This is our characteristic equation. It says that along the curve $dx/dt = c$ in space-time, the total differentials of the components of U obey

$$\mathbf{m}^{\mathrm{T}} dU = \mathbf{m}^{\mathrm{T}} G dt. \tag{2.64}$$

Each different eigenvector of A gives a different characteristic. If A has a full set of eigenvectors, as many as the components of U, then that is the number of characteristics. If A is defective and has fewer independent eigenvectors then the system is in fact not hyperbolic. The fan of characteristics going back into the past from a point (x, t) in space time covers all the points that directly influence the flow at (x, t). Adding on all the fans from those points as well fills out a cone-like region, called the domain of dependence of the point (x, t). What happened in the past at a point outside that cone cannot possibly affect conditions at (x, t).

If the system of PDEs is not in conservation-law form, we can still find the characteristics. Suppose the system is

$$M \frac{\partial U}{\partial t} + N \frac{\partial U}{\partial x} = G. \tag{2.65}$$

Then we look for generalized eigenvectors $\mathbf{m}^{\mathrm{T}}$ that obey

$$\mathbf{m}^{\mathrm{T}} N = c \mathbf{m}^{\mathrm{T}} M. \tag{2.66}$$

Given such an eigenvector, we again left-multiply the system by $\mathbf{m}^{\mathrm{T}}$ and obtain in this case

$$\mathbf{m}^{\mathrm{T}} M \left(\frac{\partial U}{\partial t} + c \frac{\partial U}{\partial x} \right) = \mathbf{m}^{\mathrm{T}} G, \tag{2.67}$$

or

$$\mathbf{m}^{\mathrm{T}} M dU = \mathbf{m}^{\mathrm{T}} G dt, \tag{2.68}$$

which, like (2.64), is a total differential equation along $dx/dt = c$.

Let's take the particular case of the Eulerian equations not in conservation-law form, viz.,

$$\frac{\partial \rho}{\partial t} + u\frac{\partial \rho}{\partial x} + \rho\frac{\partial u}{\partial x} = 0, \tag{2.69}$$

$$\frac{\partial u}{\partial t} + u\frac{\partial u}{\partial x} + \frac{1}{\rho}\frac{\partial p}{\partial x} = 0, \tag{2.70}$$

$$\frac{\partial s}{\partial t} + u\frac{\partial s}{\partial x} = 0. \tag{2.71}$$

The momentum and energy sources have been omitted for simplicity. The energy equation has been replaced by the entropy equation. (Algebraically equivalent systems of PDEs give rise to exactly the same characteristics, so we are free to do this.) If we take ρ, u, and s as the components of U, then we still need to expand the pressure derivative to get the form (2.65). The thermodynamic relations tell us that

$$dp = c^2 d\rho + (\gamma - 1)\rho T \, ds \tag{2.72}$$

for an ideal gas, where c is the adiabatic sound speed, $\sqrt{\gamma p/\rho}$.

After substituting relation (2.72) for $\partial p/\partial x$, we can write the system in the form

$$\frac{\partial}{\partial t}\begin{pmatrix} \rho \\ u \\ s \end{pmatrix} + \begin{pmatrix} u & \rho & 0 \\ c^2/\rho & u & (\gamma - 1)T \\ 0 & 0 & u \end{pmatrix}\frac{\partial}{\partial x}\begin{pmatrix} \rho \\ u \\ s \end{pmatrix} = 0. \tag{2.73}$$

We need the eigenvalues of the matrix N in the second term. Expanding the determinant of $N - v$, where is the 3×3 identity matrix, yields $(u - v)[(u - v)^2 - c^2]$. So the eigenvalues, which we will now call v to avoid confusion with the sound speed, are $v = u$ and $v = u \pm c$. The left eigenvector for $v = u$ is $(0, 0, 1)$, the one for $v = u + c$ is $(c^2, \rho c, (\gamma - 1)\rho T)$, and the one for $v = u - c$ is $(c^2, -\rho c, (\gamma - 1)\rho T)$. So our characteristic equations are

$$c^2 d\rho + \rho c\, du + (\gamma - 1)\rho T\, ds = 0 \qquad \text{on } C_+\text{:} \quad \frac{dx}{dt} = u + c, \tag{2.74}$$

$$c^2 d\rho - \rho c\, du + (\gamma - 1)\rho T\, ds = 0 \qquad \text{on } C_-\text{:} \quad \frac{dx}{dt} = u - c, \tag{2.75}$$

$$ds = 0 \qquad \text{on } C_0\text{:} \quad \frac{dx}{dt} = u. \tag{2.76}$$

We recognize the differential of the pressure in the first two equations, so we can write the system in the simpler form

$$du + \frac{dp}{\rho c} = 0 \qquad \text{on } C_+: \frac{dx}{dt} = u + c, \tag{2.77}$$

$$du - \frac{dp}{\rho c} = 0 \qquad \text{on } C_-: \frac{dx}{dt} = u - c, \tag{2.78}$$

$$ds = 0 \qquad \text{on } C_0: \frac{dx}{dt} = u. \tag{2.79}$$

In an isentropic flow the entropy is not only constant following a parcel of fluid, which is what adiabatic means and which is expressed by the C_0 characteristic equation, but is spatially uniform as well, so the entropy is everywhere and always the same (barring shocks). If this is the case, then $dp/(\rho c)$ is a total differential of the thermodynamic function

$$\int \frac{dp}{\rho c} = \frac{2c}{\gamma - 1}, \tag{2.80}$$

where the equality is valid for gamma-law gases. For this special case the first two characteristic equations are integrable, and take the form

$$r \equiv u + \frac{2c}{\gamma - 1} = \text{constant} \qquad \text{on } C_+: \frac{dx}{dt} = u + c, \tag{2.81}$$

$$l \equiv u - \frac{2c}{\gamma - 1} = \text{constant} \qquad \text{on } C_-: \frac{dx}{dt} = u - c. \tag{2.82}$$

These two functions, r and l, are called the Riemann invariants. The royal road to solving ideal gas dynamics problems of this class is to select a point where you want to know the flow variables, trace a C_+ characteristic back to the start time and evaluate r there, and this is therefore the value at the desired point. Also trace back a C_- characteristic to the start time and get l. (This tracing back may be easier said than done in some cases!) The average of r and l is the velocity at the desired point, and their difference determines the sound speed. Through the adiabatic relations, since we know the value of the entropy, we can get density, pressure, and so on.

This prescription actually works in the case of what are called simple waves. These are isentropic flows of an ideal gas for which one of the two Riemann invariants is the same everywhere. To be specific, suppose l is the same everywhere. Then consider what happens along a particular C_+ characteristic. This characteristic will have its own value of r, which will be constant along it. So on this characteristic both l and r are constant, which means that u and c are also constant, which means that the characteristic velocity is constant too. That is, this characteristic is a straight line in space-time. With different C_+ characteristics having different

values of r their slopes will differ, so they will form a fan. If the fan opens with time it is a simple rarefaction wave; if it is converging with time it is a simple compression wave. In the latter case, the characteristics eventually intersect forming a cusp, and a discontinuity, a shock, is generated at that point. This situation in which one of the Riemann invariants is constant everywhere arises when a large area has uniform density, temperature, and entropy at the initial time. The characteristics that emanate from there will carry a constant Riemann invariant when they cross into an adjacent region. The result is the theorem, "The flow adjacent to a region of constant state is a simple wave" (Courant and Friedrichs, 1948).

A simple centered rarefaction wave is an illustration of this. Suppose that a uniform block of ideal gas located at $x \leq 0$ is confined by a membrane that is removed at $t = 0$. What happens is a rarefaction wave that eats into the gas at $x < 0$ with a velocity of $-c_0$, where c_0 is the sound speed in the undisturbed gas. The gas that is disturbed moves in the $+x$ direction with a velocity that increases with x. The density drops from the undisturbed value to very small values at positive x. In this problem there is a region of constant state on the left, so the Riemann invariant r is constant everywhere, and has the value $r = 2c_0/(\gamma - 1)$. The whole region of rarefaction belongs to the fan of C_- characteristics that emanate from the point $(x, t) = (0, 0)$. This is what makes it a centered rarefaction. The slope of the C_- characteristic through the point (x, t) is the slope of the line connecting this point to $(0, 0)$, namely x/t. Thus

$$\frac{x}{t} = u - c. \tag{2.83}$$

Combining this relation with

$$r = u + \frac{2c}{\gamma - 1} = \frac{2c_0}{\gamma - 1} \tag{2.84}$$

gives

$$u = \frac{2}{\gamma + 1}\left(\frac{x}{t} + c_0\right), \tag{2.85}$$

$$c = \frac{\gamma - 1}{\gamma + 1}\left(\frac{2}{\gamma - 1}c_0 - \frac{x}{t}\right), \tag{2.86}$$

from which we can also get the density profile

$$\rho = \rho_0 \left[\frac{\gamma - 1}{\gamma + 1}\left(\frac{2}{\gamma - 1} - \frac{x}{c_0 t}\right)\right]^{2/(\gamma - 1)}, \tag{2.87}$$

with a similar relation for the pressure. We see that at any given time $t > 0$ the velocity increases linearly from 0 at the head of the rarefaction at $x = -c_0 t$ to a maximum value at the tail, $x = (2/(\gamma - 1))c_0 t$, at which point the velocity is
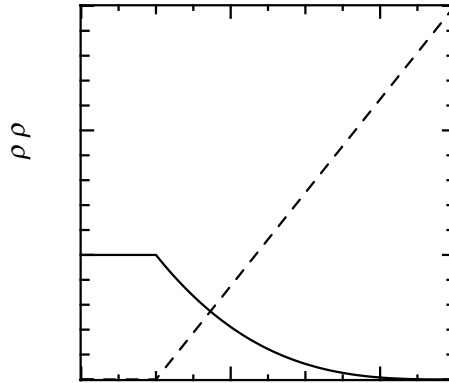
Fig. 2.2   Structure of a centered rarefaction wave. Solid line, density in units of undisturbed density; dashed line, velocity in units of undisturbed sound speed; abscissa, similarity coordinate $x/c_0 t$.

$2c_0/(\gamma - 1)$, the same as x/t. The sound speed decreases linearly from c_0 to 0 over the same interval. The density varies as c raised to the $2/(\gamma - 1)$ power; this exponent is 3 for a monatomic gas. It means the density reaches very low values as the tail is approached. These results are shown in Figure 2.2. In a Lagrangian calculation of a free rarefaction such as this, the tail may be unphysically truncated because the remaining mass is less than the mass of a single zone. The tail velocity for the free rarefaction in a monatomic gas is $3c_0$, which is a useful rule of thumb to keep in mind.

2.9 Shock waves: Rankine–Hugoniot relations

Shocks are surfaces of discontinuity of the inviscid flow equations, or represent regions interior to the flow where the viscosity and heat conduction terms are locally important – like internal boundary layers. Courant and Friedrichs (1948) develop the theory of shock waves in considerable detail. An aerodynamic rather than physical point of view is contained in Liepmann and Roshko (1957). This has a useful analysis of the shock tube problem. The excellent standard reference on hydrodynamic waves is *Linear and Nonlinear Waves* by Whitham (1974). For the outer inviscid solution shock waves are fully described by the jumps across them. Here we discuss these jump conditions – the Rankine–Hugoniot relations. We will go back to the Navier–Stokes equations and look at these in the small, in a region that includes a patch of the shock front. In a coordinate system that is comoving with the shock for a short time, the flow is almost steady. The reason is that $\mathbf{u} \cdot \nabla$ terms

are large compared with $\partial/\partial t$ terms, so the latter can be neglected. Similarly, if the shock normal is the x direction, then $\partial/\partial y$ and $\partial/\partial z$ terms are locally negligible compared with $\partial/\partial x$ terms. The assumptions need to be verified after the fact by showing that the actual shock thickness is negligible compared with length scales in the problem. The approximations allow us to treat the small region around the front using slab symmetry.

Let $\mathbf{v}$ be the flow velocity in this shock frame; it is equal to $\mathbf{u} - \mathbf{U}_s$, where $\mathbf{U}_s$ is the velocity of the shock front. (The component of $\mathbf{U}_s$ parallel to the front will turn out to be irrelevant.) We look at each of the Navier–Stokes equations in turn, and discard the time derivatives and gradients in the y and z directions. The continuity equation gives simply

$$\frac{d}{dx}(\rho v_x) = 0. \tag{2.88}$$

The Navier–Stokes momentum equation turns into

$$\frac{d}{dx}(\rho v_x \mathbf{v}) + \frac{dp}{dx}\mathbf{e}_x - \frac{d}{dx}\left[\mu\left(\frac{d\mathbf{v}}{dx} + \frac{dv_x}{dx}\mathbf{e}_x\right) + \left(\zeta - \frac{2}{3}\mu\right)\frac{dv_x}{dx}\mathbf{e}_x\right] = 0. \tag{2.89}$$

The total energy equation becomes

$$\frac{d}{dx}\left\{\rho v_x e + \frac{1}{2}\rho v_x v^2 + pv_x - \mu\left[v_x\frac{dv_x}{dx} + \frac{d}{dx}\left(\frac{1}{2}v^2\right)\right]\right.$$
$$\left. - \left(\zeta - \frac{2}{3}\mu\right)v_x\frac{dv_x}{dx} - K\frac{dT}{dx}\right\} = 0. \tag{2.90}$$

The source terms on the right-hand side of the energy and momentum equations are neglected since they are small compared with the large d/dx terms. As we see, the three conservation equations imply that three functions are constant in the flow (five, if we count the three components of momentum). In other words,

$$\rho v_x = \text{constant} = C_1, \tag{2.91}$$

$$\rho v_x^2 + p - \left(\frac{4}{3}\mu + \zeta\right)\frac{dv_x}{dx} = \text{constant} = C_2, \tag{2.92}$$

$$\rho v_x v_y - \mu\frac{dv_y}{dx} = \text{constant} = C_3, \tag{2.93}$$

$$\rho v_x v_z - \mu\frac{dv_z}{dx} = \text{constant} = C_4, \tag{2.94}$$

$$\rho v_x e + \frac{1}{2}\rho v_x v^2 + pv_x - \left(\frac{4}{3}\mu + \zeta\right)v_x\frac{dv_x}{dx}$$
$$- \mu\left(v_y\frac{dv_y}{dx} + v_z\frac{dv_z}{dx}\right) - K\frac{dT}{dx} = \text{constant} = C_5. \tag{2.95}$$

The first constant is simply the mass flux through the shock. The third and fourth equations imply that v_y and v_z are themselves constant, with the values C_3/C_1 and C_4/C_1, respectively. That enables us to discard the v_y and v_z gradient terms in the fifth equation and absorb the constant term $(1/2)\rho v_x (v_y^2 + v_z^2)$ into C_5. The modified fifth equation is

$$\rho v_x e + \frac{1}{2}\rho v_x^3 + p v_x - \left(\frac{4}{3}\mu + \zeta\right) v_x \frac{dv_x}{dx} - K\frac{dT}{dx} = \text{constant} = C_5. \quad (2.96)$$

The internal structure of shock waves is beyond the scope of these remarks, but a rough guide to the relevant length scale is provided by examining these equations. The second equation suggests that the scale in x is of order $\mu/(\rho v_x)$. Since v_x is of order the sound speed (as we will see), and μ is roughly ρ times the mean thermal speed times the mean free path, the scale in x is very roughly just the mean free path. We get the same result from the viscous term in the energy equation. If the Prandtl number is of order unity, the conclusion from the heat conduction term is the same. Now, if the shock thickness is comparable with the mean free path then *ipso facto* the fluid approximation is not accurate. The true shock structure is a problem in particle transport. In plasmas, the transport processes result in a separation of charge within the shock and a substantial electric field is created. All these complications can be significant if atomic processes such as ionization and photorecombination take place at an appreciable rate within the front. We will consider these problems no further here.

Let us then move the observation points a small distance away from the shock front on each side, so that they are far enough away from the shock for the viscosity and heat conduction terms to have become negligible, but still close compared with the main length scales of the flow. Then when we compare the three functions whose values are C_1, C_2, and C_5 between these two points, one upstream and one downstream of the shock, we get the jump conditions

$$\Delta(\rho v_x) = 0, \quad (2.97)$$

$$\Delta(p + \rho v_x^2) = 0, \quad (2.98)$$

$$\Delta\left(e + \frac{p}{\rho} + \frac{1}{2}v_x^2\right) = 0, \quad (2.99)$$

to which we can add the two we have seen already, namely $\Delta(v_y) = \Delta(v_z) = 0$. These are the Rankine–Hugoniot relations.

We might count the number of relations and compare with the number of variables. The upstream state is defined by five variables, ρ, u_x, u_y, u_z, and e. (Remember that the **v** components are $\mathbf{u} - \mathbf{U}_s$.) There are five more downstream variables, and the shock velocity U_s in the normal direction is an additional

variable. So the Rankine–Hugoniot relations give five conditions constraining the eleven unknowns. Here is how it works out that the flow is fully determined. The shock moves supersonically into the material in front of it, as we will see, so the state of that material is fully determined without any information about, or from behind, the shock. Thus the preshock values of ρ, u_x, u_y, u_z, and e are known. The jump conditions then give all the postshock values, if one more piece of information is provided. The shock velocity U_s itself is not known, and in fact the shock may speed up or slow down in response to what the flow is doing. The extra piece of information is the one that is carried along the forward characteristic in the postshock region; this characteristic overtakes the shock from behind since the shock moves subsonically with respect to the region behind it. Thus the preshock conditions, plus the one piece of information from the postshock flow, determine all the postshock flow variables, and also the shock velocity.

A number of important results emerge from manipulation of the jump conditions, such as the property mentioned already that the shock propagates supersonically with respect to the gas in front and subsonically with respect to the gas behind. In the presentation below we use the notation v_0, ρ_0, p_0, etc., for quantities in front of the shock, and a subscript 1 for quantities behind the shock. The specific volume, $1/\rho$, will be denoted by V. The mass conservation relation becomes

$$v_0 = C_1 V_0 \quad \text{and} \quad v_1 = C_1 V_1, \tag{2.100}$$

so

$$\frac{V_0}{V_1} = \frac{v_0}{v_1}. \tag{2.101}$$

Since

$$p_0 + C_1^2 V_0 = p_1 + C_1^2 V_1, \tag{2.102}$$

the mass flux is given by

$$C_1 = \sqrt{\frac{p_1 - p_0}{V_0 - V_1}}, \tag{2.103}$$

and therefore the pre- and post-shock flow speeds with respect to the shock are

$$v_0 = V_0 \sqrt{\frac{p_1 - p_0}{V_0 - V_1}} \tag{2.104}$$

and

$$v_1 = V_1 \sqrt{\frac{p_1 - p_0}{V_0 - V_1}}. \tag{2.105}$$

Therefore the velocity jump is

$$v_0 - v_1 = \sqrt{(p_1 - p_0)(V_0 - V_1)}, \tag{2.106}$$

and the kinetic energy jump is

$$\frac{1}{2}v_0^2 - \frac{1}{2}v_1^2 = \frac{1}{2}(p_1 - p_0)(V_0 + V_1), \tag{2.107}$$

which, because of the energy jump condition, also gives the enthalpy jump:

$$h_1 - h_0 = \frac{1}{2}(p_1 - p_0)(V_0 + V_1). \tag{2.108}$$

Subtracting $p_1 V_1 - p_0 V_0$ from both sides gives the internal energy jump:

$$e_1 - e_0 = \frac{1}{2}(p_1 + p_0)(V_0 - V_1). \tag{2.109}$$

(Notice the $+$ and $-$ switched!) The set of all thermodynamic states P_1, V_1 that satisfy either of the last two equations for a specific initial state p_0, V_0 defines the Hugoniot curve for that state.

Using the ideal gas law all the relations can be made explicit. For the ideal gas,

$$e = \frac{PV}{\gamma - 1}, \tag{2.110}$$

so the Hugoniot equation (2.109) can be solved for the pressure ratio to give

$$\frac{p_1}{p_0} = \frac{(\gamma + 1)V_0 - (\gamma - 1)V_1}{(\gamma + 1)V_1 - (\gamma - 1)V_0}. \tag{2.111}$$

This is the equation of a hyperbola in the P, V diagram. The vertical asymptote is at

$$\frac{V_0}{V_1} = \frac{\rho_1}{\rho_0} = \frac{\gamma + 1}{\gamma - 1}, \tag{2.112}$$

which therefore is the maximum possible compression in a single shock. This ratio is 4 for a monatomic gas, for which $\gamma = 5/3$. The horizontal asymptote is

$$\frac{p_1}{p_0} = -\frac{\gamma - 1}{\gamma + 1}. \tag{2.113}$$

The curve crosses the V axis at

$$\frac{V_1}{V_0} = \frac{\gamma + 1}{\gamma - 1}. \tag{2.114}$$

Of course, values of V_1 that are larger than V_0 represent expansion, which cannot occur in a shock. The Mach number equations are

$$M_0^2 \equiv \left(\frac{v_0}{c_0}\right)^2 = \frac{(\gamma - 1) + (\gamma + 1)p_1/p_0}{2\gamma} \tag{2.115}$$

and

$$M_1^2 \equiv \left(\frac{v_1}{c_1}\right)^2 = \frac{(\gamma - 1) + (\gamma + 1)p_0/p_1}{2\gamma}. \tag{2.116}$$

Since $p_1 > p_0$, $M_0 > 1$ and $M_1 < 1$, substantiating the earlier claim that preshock flow is supersonic and postshock flow is subsonic, at least for ideal gases. The relation is also true for a general equation of state, although the proof is more subtle in that case.

The entropy jump is

$$s_1 - s_0 = \frac{e_0}{T_0} \log\left[\frac{p_1}{p_0}\left(\frac{(\gamma - 1)p_1/p_0 + (\gamma + 1)}{(\gamma + 1)p_1/p_0 + (\gamma - 1)}\right)^\gamma\right]. \tag{2.117}$$

This is positive for all shocks. It is 0 for $p_1 = p_0$, the limit of a weak shock, and increases indefinitely as $p_1/p_0 \to \infty$. It remains very small for modest values of $p_1/p_0 - 1$, and is proportional to the cube of $p_1/p_0 - 1$ (or of $M_0 - 1$) for weak shocks.

The jump conditions for a strong shock are often used as a limiting case. Besides the density jump

$$\rho_1 = \frac{\gamma + 1}{\gamma - 1}\rho_0 \tag{2.118}$$

that we saw before, the other two relations are

$$v_1 = \frac{\gamma - 1}{\gamma + 1}v_0 \tag{2.119}$$

and

$$p_1 = \frac{2\gamma}{\gamma + 1}\frac{v_0^2}{c_0^2}p_0 = \frac{2}{\gamma + 1}\rho_0 v_0^2. \tag{2.120}$$

The internal energy behind a strong shock is

$$e_1 = \frac{p_1}{(\gamma - 1)\rho_1} = \frac{4}{(\gamma + 1)^2}\frac{1}{2}v_0^2; \tag{2.121}$$

the enthalpy is

$$h_1 = \frac{4\gamma}{(\gamma+1)^2} \frac{1}{2} v_0^2. \tag{2.122}$$

Thus a large fraction of the kinetic energy entering the shock is turned into heat, but not all of it, since there is still residual kinetic energy in the flow behind the shock. For the $\gamma = 5/3$ gas, the postshock internal energy is 9/16 of the incoming kinetic energy, and the enthalpy is 15/16 of the incoming kinetic energy.

2.10 The Taylor–Sedov blast wave

This is the classical example that demonstrates a self-similar solution of a gas dynamic problem. The discussion here follows Landau and Lifshitz (1959), but the reader should be beware of typographical errors in the first edition, mentioned below. There is a good discussion, lacking the mathematical details, in Zel'dovich and Raizer (1967). The blast wave is also discussed, without typographical errors, in Sedov (1959), the classic of similarity methods. Consider an infinite space filled with a gas at rest at a uniform density, ρ_0, with negligible pressure. At $t = 0$ a certain amount of energy E is deposited in a tiny region at the origin. The details of how the energy is distributed between thermal and kinetic, and the spatial distribution of the deposited energy within the tiny volume, are soon forgotten. One significant point is that the amount of extra mass in the tiny volume, above the amount expected from the ambient density, is not large enough to be important. What follows is an expanding spherical shock front, behind which is a radial distribution of density, pressure, and velocity. The idea of self-similarity is that the radial distributions at different times are scalable. That is, they are the same if the radial scale and the scale of the variable are stretched appropriately. The scale transformations in self-similar problems often follow from dimensional analysis, as they do in this case.

The only data for this problem are the ambient density ρ_0 and the energy, E. At a certain time t the three quantities ρ_0, E, and t can be used to construct combinations with the dimensions of radius, velocity, and pressure. These are

$$r_1 = \left(\frac{Et^2}{\rho_0} \right)^{1/5}, \tag{2.123}$$

$$u_1 = \frac{2}{\gamma+1} \xi_0 \frac{dr_1}{dt} = \frac{4}{5} \frac{\xi_0}{\gamma+1} \left(\frac{E}{t^3 \rho_0} \right)^{1/5}, \tag{2.124}$$

$$p_1 = \frac{2}{\gamma+1} \rho_0 \left(\xi_0 \frac{dr_1}{dt} \right)^2 = \frac{8}{25} \frac{\xi_0}{(\gamma+1)^2} \left(\frac{E^2 \rho_0^3}{t^6} \right)^{1/5}. \tag{2.125}$$

The reason for the extra numerical factors in these expressions will become apparent shortly. The similarity assumption is that the scaled variables

$$\tilde{u} = \frac{u}{u_1}, \tag{2.126}$$

$$\tilde{p} = \frac{p}{p_1}, \tag{2.127}$$

$$\tilde{\rho} = \frac{\gamma - 1}{\gamma + 1} \frac{\rho}{\rho_0} \tag{2.128}$$

are functions only of the scaled radius

$$\xi = \frac{r}{r_1} \tag{2.129}$$

and not of radius and time separately.

These substitutions are made into the Euler equations and, if we have done our work correctly and the problem is really self-similar, the factors involving E, ρ_0, and t all cancel out, and we are left with three ordinary differential equations in ξ for the unknowns $\tilde{u}$, $\tilde{p}$, and $\tilde{\rho}$. The location of the shock in the ξ coordinate, ξ_0, is to be determined. Given a value for ξ_0, the jump conditions (for a strong shock $p_1 \gg p_0$) determine the values of $\tilde{u}$, $\tilde{p}$, and $\tilde{\rho}$ at that point, just behind the shock. The factors introduced in the definitions of u_1 and p_1 above, and in the definition of $\tilde{\rho}$, are based on the jump conditions, and lead to the values at $\xi = \xi_0$

$$\tilde{u} = \tilde{p} = \tilde{\rho} = 1. \tag{2.130}$$

Inward radial integrations give a provisional structure. But the integral of the total kinetic and internal energy within the shocked region does not necessarily equal E; the value of ξ_0 is adjusted to make it so. The details of the analytic integration of the equations are given by Landau and Lifshitz (1959). (Users of the first edition of the Landau and Lifshitz reference should be aware of typographical errors: the exponent ν_5 in [99.10] should be $2/(\gamma - 2)$, not $1/(\gamma - 2)$, and the power of ξ multiplying p' in [99.11] should be 4 not 9. Furthermore, the variable ξ for all the terms in the integral in [99.11], and the integration variable, should be ξ/ξ_0.)

The results for the $\gamma = 5/3$ case are that $\xi_0 = 1.152$, and the distributions of u, p, and ρ are as shown in Figure 2.3. Some interesting features of the solution are that the velocity is almost linear in r, which is the ballistic relation $v = r/t$. The pressure drops steeply behind the shock, but only by a factor of about 2.5, and is nearly constant over most of the sphere. The density has a very large dynamic range. The inner part of the sphere is almost totally evacuated, and the mass that formerly occupied the volume of the sphere has been packed into a thin shell behind the shock. The temperature and entropy, not shown in the figure, are much larger near the center than just behind the shock. That is because each parcel of
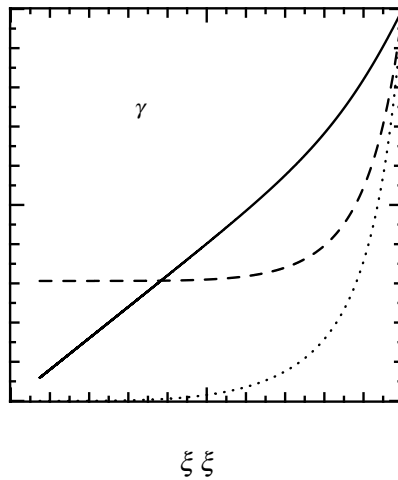
Fig. 2.3 Structure of the $\gamma = 5/3$ blast wave. The ordinates are: solid curve, scaled velocity; dashed curve, the scaled pressure; dotted curve, the scaled density, as defined in (2.126)–(2.128) in the text. The abscissa is the scaled radius ξ defined in (2.129).

material remembers how strong the shock was when it passed through the shock. (The entropy of a parcel is preserved in inviscid flow, apart from shocks.) At early time the shock is stronger and the entropy increase is correspondingly larger than at later time; this maps into an increase of entropy, and therefore of temperature, toward the center.

2.11 The shock tube

One of the best shock wave examples, often used as a test problem, is the shock tube. This is a model of a laboratory experiment in which a long gas cell initially contains a high-pressure gas on one side of a membrane and a much lower-pressure gas on the other side, possibly of a different temperature or composition. At time 0 the membrane is removed. What results is a shock wave propagating into the low-pressure gas, followed by a region of constant state made up of the initially low-pressure gas. This joins another constant-state region made up of initially high-pressure gas, but these two constant-state regions have the same pressure and velocity at this point. Next is a rarefaction progressing into the high-pressure region. Beyond the rarefaction on one side and beyond the shock on the other side are the undisturbed high- and low-pressure gases. The analysis of the shock tube demonstrates several of the methods of compressible gas dynamics.

The solution for a typical shock tube problem is shown in Figure 2.4. We suppose that the high-pressure region is to the left, and the low-pressure region is to the right. The four regions of constant state are numbered 1 through 4 going from left to right: 1 is the undisturbed high-pressure gas, 2 is the region of expanded initially high-pressure gas, 3 is the region of shocked initially low-pressure gas, and 4 is the region of undisturbed low-pressure gas. Coordinate x_1 is the head of the rarefaction wave; x_2 is the tail of the rarefaction; x_3 is the contact discontinuity separating what was once high-pressure material from what was once low-pressure material; and x_4 is the location of the shock.

A contact discontinuity has to satisfy jump conditions just as a shock does, but these are very simple. There is no flow through the discontinuity, so the fluid velocity on each side is the same as the velocity of the discontinuity; the fluid velocity therefore must be continuous. The pressure jump condition reduces in the case that there is no flow across the interface to the statement that the pressure is continuous. The energy jump condition is automatically satisfied if the first two conditions are obeyed.

For the shock tube this means that constant-state regions 2 and 3 share the same velocity and pressure. The densities and sound speeds can be, and indeed will be, different, however. The first step in the procedure for solving a shock tube is to find the pressure and velocity in regions 2 and 3. The pressure will be intermediate between the initial values p_1 and p_4, and the velocity will be some positive value. The method of solution is to use the centered rarefaction relations to express the velocity difference across the rarefaction, which will be u_2, as a function of the unknown pressure ratio p_1/p_2. Likewise the shock jump conditions are used to express the velocity jump across the shock, which will be u_3, as a function of the pressure ratio p_3/p_4. But u_2 and u_3 must be the same, and p_2 and p_3 are the same, so p_3/p_4 can be expressed as $(p_1/p_4)/(p_1/p_2)$. The ratio p_1/p_4 is one of the data for the problem, so there is a single unknown, p_1/p_2. The equation $u_2 = u_3$ becomes an algebraic equation for p_1/p_2. This has to be solved numerically. Here is the equation when we allow the two gases to have different γs:

$$\frac{2c_1}{\gamma_1 - 1} \left[1 - (p_2/p_1)^{(\gamma_1-1)/(2\gamma_1)} \right] = \frac{\sqrt{2}c_4(p_3/p_4 - 1)}{\sqrt{\gamma_4[\gamma_4 - 1 + (\gamma_4 + 1)p_3/p_4]}}, \quad (2.131)$$

where p_3/p_4 is to be replaced by $(p_1/p_4)/(p_1/p_2)$. In practice we use a root-finder method such as Newton–Raphson to find the solution. Once this equation has been solved, the left- or the right-hand side gives the value of u_2, and the adiabatic relation across the rarefaction gives ρ_2 and c_2. Other shock jump conditions give ρ_3 and the shock velocity U_s since p_3/p_4 is known.

The spatial structure of the shock tube solution is self-similar in time, since all the variables are functions of x/t, assuming that the initial membrane location was
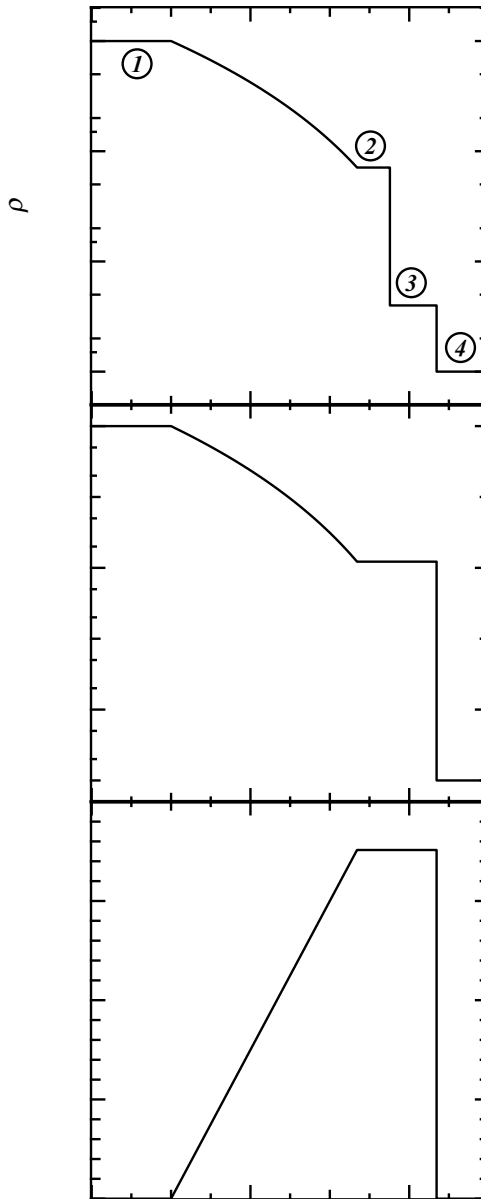
Fig. 2.4   Structure for the shock tube described in the text. Abscissa, x/t; ordinate, density (top), pressure (middle) and velocity (bottom). The four regions discussed in the text are indicated on the density curve.

$x = 0$. The locations of the four features can easily be read off. The x coordinate of the shock is x_4, which is given by $x_4/t = U_s$. The x coordinate of the contact discontinuity is x_3, which is given by $x_3/t = u_2$. The x coordinate of the head of the rarefaction is x_1, which is given by $x_1/t = -c_1$, and the x coordinate of the tail is x_2, which is given by $x_2/t = u_2 - c_2$. That defines everything except the shape of the rarefaction wave. As in the example of a free rarefaction, this is a simple wave, and the Riemann invariant r is constant throughout the wave. Following the same algebra as above (see (2.83)–(2.86)) leads to the results

$$u = \frac{2}{\gamma_1 + 1} \left(\frac{x}{t} + c_1 \right), \tag{2.132}$$

$$c = \frac{2c_1}{\gamma_1 + 1} - \frac{\gamma_1 - 1}{\gamma_1 + 1} \frac{x}{t}, \tag{2.133}$$

for x/t in the range $-c_1 < x/t < u_2 - c_2$. The pressure and density distributions are then derived from c using the adiabatic relations connecting each point with region 1.

Obtaining this solution with acceptable accuracy is found to be a challenging test for numerical hydrodynamics codes, particularly when extreme values are chosen for the pressure ratio p_1/p_4. Eulerian codes may have problems smearing out the contact discontinuity, and Lagrangian codes sometimes do not do well with the rarefaction wave because the Lagrangian zones end up being poorly distributed in the x coordinate because of the large density variation. Both codes sometimes will have ringing on one side or the other of the shock jump.

Figure 2.4 shows a shock tube with a pressure ratio of 10^5:1 and a density ratio of 10^3:1 with $\gamma = 5/3$ gases on both sides. The solution of the shock tube equation gives $p_2/p_1 = 0.0122$ so the pressure ratio across the shock is 1222. The shock Mach number turns out to be 23.4, which makes it a very strong shock. As expected in this case, the density ratio ρ_3/ρ_4, 3.988, is very close to the limiting value 4. The density ratio across the contact is large, 17.8:1. This means that the shocked gas is much hotter than the rarefied former high-pressure gas, even though the latter began 100 times hotter than the low-pressure gas.